

Experimental Manifestations of Fermion Condensation in Strongly Correlated Fermi Systems

V.A. STEPHANOVICH^{a*}, V.R. SHAGINYAN^b AND E.V. KIRICHENKO^c

^aInstitute of Physics, Opole University, Oleska 48, 45-052 Opole, Poland

^bPetersburg Nuclear Physics Institute of NRC “Kurchatov Institute”, Gatchina, 188300, Russia

^cInstitute of Mathematics and Informatics, Opole University, Oleska 48, 45-052 Opole, Poland

Many strongly correlated Fermi systems including heavy-fermion (HF) metals and high- T_c superconductors belong to that class of quantum many-body systems for which the Landau–Fermi liquid theory fails. Instead, these systems exhibit non-Fermi-liquid properties that arise from violation of time-reversal (T) and particle–hole (C) invariance. Here we consider two most recent experimental puzzles, which cannot be explained neither within the Landau–Fermi liquid picture nor can they be made intelligible by the approaches like the Hubbard model and/or the Kondo effect, which are commonly used to spell out the typical non-Fermi-liquid behavior. The first experimental puzzle is the asymmetric (with respect to bias voltage V) tunneling conductance (more specifically differential conductivity dI/dV , where I is the current) of HF metals like CeCoIn₅ and YbRh₂Si₂ and Leggett theorem violation in overdoped copper HTSC oxides. The second puzzle is strange properties of geometrically frustrated 2D magnets like herbertsmithite ZnCu₃(OH)₆Cl₂, of which unusual properties are related to the emergence of so-called quantum spin liquid formed from fermionic spinons — the quasiparticles which substitute ordinary bosonic magnons in geometrically frustrated substances. It turns out that in both above classes of compounds, the background Fermi liquid (quantum spin liquid in geometrically frustrated magnets and electron liquid in other substances) is considered to undergo a transformation that renders a portion of its excitation spectrum dispersionless, giving rise to so-called flat bands. The presence of a flat band indicates that the system is close to a special quantum critical point, namely a *topological fermion-condensation quantum phase transition*. An essential aspect of the behavior of a system hosting a flat band is that application of a magnetic field restores its normal Fermi-liquid properties, including T- and C-invariance, thus removing above non-Fermi-liquid anomalies.

DOI: [10.12693/APhysPolA.135.1204](https://doi.org/10.12693/APhysPolA.135.1204)

PACS/topics: strongly correlated fermions, fermion condensation, heavy-fermion compounds, Leggett theorem

1. Introduction

Many strongly correlated Fermi systems, notably those electronic solids identified as heavy-fermion (HF) metals and high- T_c superconductors (HTSC), belong to a new class of materials for which standard Landau–Fermi liquid (LFL) theory no longer applies. Instead, the systems demonstrate so-called non-Fermi-liquid (NFL) properties, typically reflecting violation of time-reversal and particle–antiparticle invariances (respectively T-invariance and C-invariance). Measurement of tunneling conductance provides a powerful experimental technique for detecting these symmetry violations. Preservation of T and C symmetries is inherent in LFL theory, which implies that the differential conductivity formed from the current I and bias voltage V is necessarily a symmetric function of V . It has been predicted that the conductivity becomes asymmetric for HF metals such as CeCoIn₅ and YbRh₂Si₂. As an underlying mechanism, it is posited in these materials that the electronic system undergoes a special kind of transformation: a portion of its single-particle spectrum becomes dispersionless, forming a so-called flat band and leading to the asymmetrical conductivity [1–4]. Emergence of a flat band implies that the

system possesses a quantum critical point representing a topological instability. This instability induces a topological fermion-condensation quantum phase transition (FCQPT) [3, 5, 6] involving the phenomenon of fermion condensation (FC). Importantly, application of a magnetic field B restores the usual Fermi-liquid properties, i.e., the differential conductivity becomes a symmetric function of V due to the reappearance of the T- and C-invariances [1–3]. This behavior has been observed in recent measurements of tunneling conductivity on both YbRh₂Si₂ [7, 8] and graphene [9].

Analysis of the data [8, 9] provides an explicit demonstration of the restoration of symmetry. In a geometrically frustrated magnet, spins are prevented from forming an ordered alignment, so that even at temperatures close to absolute zero they occupy a liquid-like state called a quantum spin liquid (QSL). The herbertsmithite mineral has been exposed as a $S = 1/2$ kagome antiferromagnet, and recent experimental investigations have revealed its unusual behavior [10–15]. The balance of electrostatic forces for the Cu²⁺ ions in the kagome structure is such that they occupy distorted octahedral sites. The magnetic planes formed by the Cu²⁺ $S = 1/2$ ions are interspersed with nonmagnetic Zn²⁺ layers. In samples, Cu²⁺ defects occupy the nonmagnetic Zn²⁺ sites between the kagome layers with $x \simeq 15\%$ probability, thus introducing randomness and inhomogeneity into the lattice [16]. As we shall see, the starring role of impurities

*corresponding author; e-mail: stef@uni.opole.pl

in formation of the QSL is not clearly understood. However, we suggest that the influence of impurities induced by the homogeneity on the properties of $\text{ZnCu}_3(\text{OH})_6\text{Cl}_2$ can be tested by varying x . We note that the impurities can stabilize QSL as it is observed in measurements on the verdazyl-based complex $\text{Zn}(\text{hfac})_2(\text{A}_x\text{B}_{1-x})$ [17]. The experiments made on $\text{ZnCu}_3(\text{OH})_6\text{Cl}_2$ have not found any traces of magnetic order in it. Nor have they found the spin freezing down to temperatures of around 50 mK. In these respects, herbertsmithite is the best candidate among quantum magnets to contain the QSL described above [10–15]. These assessments are supported by model calculations indicating that the ground state of kagome antiferromagnet is a gapless spin liquid [3, 6, 18–23].

On the other hand, the recent studies suggest that there can exist a small spin-gap in the kagome layers that stands in conflict to this emerging picture [16, 24, 25] (see also Refs. [26–28] for a recent review). The results reported are based on both experimental findings and their theoretical interpretation in the framework of the impurity model. The experimental data involved are derived from high-resolution low-energy inelastic neutron scattering on $\text{ZnCu}_3(\text{OH})_6\text{Cl}_2$ single crystals. It is assumed that the influence of the Cu impurity ensemble on the observed properties of herbertsmithite may be disentangled from that of the kagome lattice geometry [16, 24, 25].

It is further assumed that the impurity ensemble may be represented as a simple cubic lattice in the dilute limit below the percolation threshold. The model then assumes that the spin gap survives under the application of magnetic fields up to 9 T [24], while in the absence of magnetic fields the bulk spin susceptibility χ exhibits a divergent Curie-like tail, indicating that some of the Cu spins act like weakly coupled impurities [16, 24, 25]. The same behavior is recently reported in a new kagome quantum spin liquid candidate $\text{Cu}_3\text{Zn}(\text{OH})_6\text{FBr}$ [29]. As a result, we observe a challenging contradiction between two sets of experimental data when some of them state the absent of a gap, while the other present evidences in the favor of gap.

In many common superconductors, the density n_s of superconducting electrons is equal to the total electron density n_t , as a manifestation of a well-known theorem of Leggett [30, 31]. However, recent measurements on overdoped copper HTSC oxides have demonstrated the putatively anomalous behavior $n_s \ll n_t$, awaiting explanation. In other words, the density of paired (superfluid) charge carriers turns out to be much lower than that predicted by the standard theory of Bardeen, Cooper, and Schrieffer (BCS) for conventional superconductors, within which n_s is directly proportional to the critical temperature T_c over a wide doping range [32, 33]. Broadly speaking, if no conventional explanation of this behavior can be given, such a departure from BCS theory may occur because the electronic fluid within the material is not a normal Fermi liquid in the sense of Landau FL theory.

More specifically, the system may exhibit a FCQPT, beyond which some charge carriers form a fermion condensate (FC) having very exotic properties [3, 6]. In particular, the Leggett theorem no longer applies [34], since the T- and C-invariances are violated in systems exhibiting a FC [3, 6, 35].

Also of special interest as possible expressions of new physics are observations involving resistivity ρ and zero temperature London penetration depth λ_0 that indicate a universal scaling property

$$\frac{d\rho}{dT} \propto \lambda_0^2 \quad (1)$$

for a large number of strongly correlated high-temperature superconductors [36]. This scaling relation spans several orders of magnitude in λ , attesting to the robustness of the empirical law (1); indeed, the behavior is similar to that documented in Ref. [37] and explained in Ref. [38]. We shall show that the observed scaling is simply explained by the emergence of flat bands formed by fermion condensation [39, 40].

Here we are going to show that both above groups of substances have one very important similarity — their basic physical properties are determined by the fermion condensate (and corresponding topological phase transition) emerging due to presence of the flat band in the energy spectra of their fermionic quasiparticles.

2. Fermion condensation

For decades, the famous Landau–Fermi liquid (LFL) theory [41] has been de facto the universal tool to describe the itinerant fermionic systems. It describes the ensemble of interacting electrons and nuclei in a solid in terms of a weakly interacting quasiparticle gas. This implies that the elementary excitations behave like these quasiparticles, determining the low-temperature physical properties of the system under consideration. The quasiparticles have a certain effective mass M^* , which is a parameter of the theory [41–43], being approximately independent of external stimuli including temperature, pressure, or an electromagnetic field. The LFL theory cannot, however, explain experimental results related to a strong dependence of the effective mass M^* on temperature or magnetic field, as observed in strongly correlated Fermi systems [3, 44]. At the same time, deviations from LFL behavior are observed in the vicinity of a FCQPT [3, 44]. These so-called non-Fermi-liquid anomalies are generated by large value of the effective mass (infinite at a FCQPT point; see [3, 6] for details).

We now outline the physical mechanism responsible for the dependence of the Landau quasiparticle effective mass, $M^*(B, T)$, on magnetic field and temperature. Again, the key point is that upon approach to the FCQPT from the LFL regime, the effective mass begins to depend strongly on temperature T , magnetic field B , and other external parameters such as the pressure P [3]. In effect, this phenomenon is directly related to the existence of an additional instability channel for

the Landau–Fermi liquid, in addition to the well-known Pomeranchuk instability channel (see e.g., Ref. [42]), the new channel being activated when the effective mass approaches infinity.

To avoid unphysical situations related, for instance, to the negativity of the effective mass, the system alters the topology of its Fermi surface [5, 40], such that the effective mass acquires temperature and magnetic field dependences [3]. To investigate the low-temperature transport properties, scaling behavior, and effective mass $M^*(B, T)$ of a fermionic ensemble, we adopt the model of homogeneous Fermi liquid. In that case, the description avoids complications associated with the crystalline anisotropy of solids [3], and the Landau equation for effective mass M^* of a quasiparticle, in the presence of a magnetic field of strength B , now reads [3, 41]:

$$\frac{1}{M^*(B, T)} = \frac{1}{M} + \sum_{\sigma_1} \int \frac{\mathbf{p}_F \cdot \mathbf{p}}{p_F^3} F(\mathbf{p}_F, \mathbf{p}) \times \frac{\partial n_{\sigma_1}(\mathbf{p}, T, B)}{\partial p} \frac{d\mathbf{p}}{(2\pi)^3}. \quad (2)$$

In this expression, M is the bare mass, $F(\mathbf{p}_F, \mathbf{p})$ is the Landau interaction function, which depends here on the Fermi momentum p_F and momentum p , and $n_{\sigma}(\mathbf{p}, T, B)$ is the quasiparticle distribution function for spin projection σ . The quasiparticle interaction $F(\mathbf{p}, \mathbf{p}_1)$, assumed here to be spin-independent, is phenomenological, being chosen to provide the best fit to experiment, and σ is the spin index. For simplicity, we assume that the Landau interaction does not depend on temperature so that the quasiparticle distribution has the Fermi–Dirac form

$$n_{\sigma}(\mathbf{p}, T) = \left[1 + \exp\left(\frac{\varepsilon_{\sigma}(\mathbf{p}, T) - \mu_{\sigma}}{T}\right) \right]^{-1}, \quad (3)$$

in terms of the single-particle energy spectrum $\varepsilon_{\sigma}(\mathbf{p}, T)$. In the case under consideration, the chemical potential μ depends on the spin through the Zeeman splitting $\mu_{\sigma} = \mu \pm \mu_B B$, where μ_B is the Bohr magneton. In the LFL theory, the single-particle spectrum is obtained as a variational derivative of the system energy $E[n_{\sigma}(\mathbf{p}, T)]$:

$$\varepsilon_{\sigma}(\mathbf{p}, T) = \frac{\delta E[n(\mathbf{p})]}{\delta n_{\sigma}}.$$

In describing of strongly correlated fermion ensembles, the choice of the shape and parameters of the interaction function $F(\mathbf{p}, \mathbf{p}_1)$ is dictated by its possession of an FCQPT [3]. Thus, the role of the Landau interaction is to bring the system to the FCQPT point, at which the topology of the Fermi surface is altered in such a way that the effective mass acquires temperature and field dependence [3]. The variational principle, applied to the functional $E[n_{\sigma}(\mathbf{p}, T)]$, leads to the following explicit expression for $\varepsilon_{\sigma}(\mathbf{p}, T)$:

$$\frac{\partial \varepsilon_{\sigma}(\mathbf{p}, T)}{\partial \mathbf{p}} = \frac{\mathbf{p}}{M} - \int \frac{\partial F(\mathbf{p}, \mathbf{p}_1)}{\partial \mathbf{p}} n_{\sigma}(\mathbf{p}_1, T) \frac{d^3 p_1}{(2\pi)^3}, \quad (4)$$

Equations (3) and (4) provide for self-consistent determination of $\varepsilon_{\sigma}(\mathbf{p}, T)$ and $n_{\sigma}(\mathbf{p}, T)$, yielding in turn the effective mass through $p_F/M^* = \partial \varepsilon(p)/\partial p|_{p=p_F}$. At the FCQPT point, Eq. (2) can be solved analytically [3]. At $B = 0$, contrary to LFL case, where the effective mass is approximately constant, M^* now becomes strongly temperature dependent, demonstrating the NFL behavior

$$M^*(T) \simeq a_T T^{-2/3}. \quad (5)$$

At finite T , the system undergoes a transition to the LFL region of the phase diagram, and being subjected to the magnetic field, exhibits the behavior

$$M^*(B) \simeq a_B B^{-2/3} \quad (6)$$

of the effective mass.

The introduction of “internal” (or natural) scales greatly simplifies analysis of the problem under consideration. We first observe that near the FCQPT, the solution $M^*(B, T)$ of Eq. (2) reaches its maximal value M_M^* at certain temperature $T_M \propto B$ [3]. Hence, to measure the effective mass and temperature, it is convenient to introduce the scales M_M^* and T_M , respectively. This generates the normalized effective mass $M_N^* = M^*/M_M^*$ and temperature $T_N = T/T_M$. Close to the FCQPT, the normalized solution $M_N^*(T_N)$ of Eq. (2) is well approximated by a simple universal interpolating function [3]. The interpolation occurs between the LFL and NFL states, reflecting the universal scaling behavior of M_N^* [3]:

$$M_N^*(y) \approx c_0 \frac{1 + c_1 y^2}{1 + c_2 y^{8/3}}. \quad (7)$$

Here $y = T_N = T/T_M$ and $c_0 = (1 + c_2)/(1 + c_1)$, where c_1 and c_2 are free parameters. The magnetic field B enters Eq. (2) only in the combination $\mu_B B/T$, making $T_M \sim \mu_B B$. It follows from Eq. (7) that

$$T_M \simeq a_1 \mu_B B, \quad (8)$$

where a_1 is a factor and μ_B is the Bohr magneton. Thus, in the presence of a magnetic field the variable y becomes $y = T/T_M \sim T/\mu_B B$. Based on Eq. (8) we may conclude that Eq. (7) describes the scaling behavior of the effective mass as a function of T and B . Thus the curves M_N^* at different magnetic fields B merge into a single one when expressed in terms of the normalized variable $y = T/T_M$. Since the variables T and B enter symmetrically, Eq. (7) also describes the scaling behavior of $M_N^*(B, T)$ as a function of B at fixed T .

3. Thermodynamic properties of geometrically frustrated magnets

To analyze theoretically the QSL in herbertsmithite and other geometrically frustrated magnets, we employ the strongly correlated quantum spin liquid (SC-QSL) [3, 18, 20, 23] model. A simple kagome lattice may host a dispersionless topologically protected branch of the quasiparticle spectrum with zero excitation energy, known as a flat band [3, 5, 18, 23]. In that case the FCQPT can be considered as a quantum critical point (QCP) of the $\text{ZnCu}_3(\text{OH})_6\text{Cl}_2$ QSL composed of fermions — spinons — with zero charge, occupying the

corresponding Fermi sphere with the Fermi momentum p_F and the effective mass M^* [3, 5, 6]. Consequently, the properties of geometrically frustrated magnets coincide with those of heavy-fermion metals with one exception, namely the typical insulator resists the electric current flow [18–20].

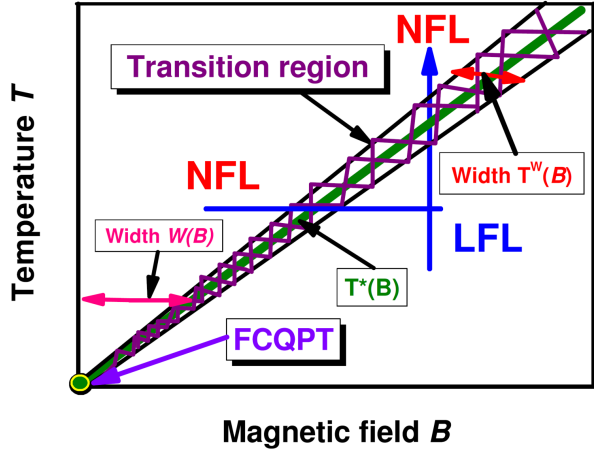


Fig. 1. Schematic SCQSL phase diagram in the “temperature-magnetic field” representation. Vertical and horizontal arrows show LFL-NFL and NFL-LFL transitions at fixed B and T , respectively. The hatched area represents the transition region at $T = T^*(B)$, see Eq. (9). The solid line in the hatched area represents the function $T^*(B) \simeq T_M(B)$ given by Eq. (8). The functions $W(B) \propto T \propto T^*$ and $T^W(B) \propto T \propto T^*$ shown by two-headed arrows define the width of the NFL state and the transition area, respectively. At FCQPT point (origin) the effective mass M^* diverges and both $W(B)$ and $T^W(B)$ tend to zero.

The above information permits us already to construct the schematic phase diagram in terms of SCQSL. It is reported in Fig. 1. For simplicity we assume that at $T = 0$ and $B = 0$ the system is approximately located at FCQPT without tuning. The external stimuli B and T are indeed the control parameters, shifting the system from FCQPT and driving it from the NFL to LFL regions as shown by the vertical and horizontal arrows. At fixed temperatures the increase of B drives the system along the horizontal arrow from the NFL to LFL region. At fixed magnetic field and increasing temperatures the system transits along the vertical arrow from the LFL to the NFL part of the phase diagram. The hatched area indicating the transition region, separates the NFL and LFL states. The transition temperature $T^*(B)$ is given by

$$T^*(B) \simeq T_M(B), \quad (9)$$

which directly follows from Eq. (8). The solid line represents the condition $T^*(B) \simeq T_M(B)$. Referring to Eq. (9), this line is defined by the function $T^* \propto \mu_B B$, and the width $W(B)$ of the NFL state is seen to be proportional to T . In the same way, it can be shown that the width $T^W(B)$ of the transition region is also proportional

to temperature [3]. We note here that in essence the transition region represents the crossover between LFL and NFL phases. In our case, the NFL phase is formed by quasiparticles that occupy the FC state, in analogy to the Bose condensate for particles obeying the Bose–Einstein statistics, see Ref. [6] for a comprehensive explanation. In a “pure” FC state, all fermions (quasiparticles) having momenta in a finite interval embracing the Fermi surface have energies pinned to the chemical potential. In reality this state cannot be reached because of the Nernst theorem [45], and the NFL features arise from “traces” of the FC state manifested at finite temperatures. Also, at low but finite temperatures, the magnetic field suppresses NFL behavior (i.e., the “FC traces”) and, on growing sufficiently strong, restores the LFL phase. On the other hand, thermal fluctuations destroy LFL behavior and generate NFL features related to the FC state.

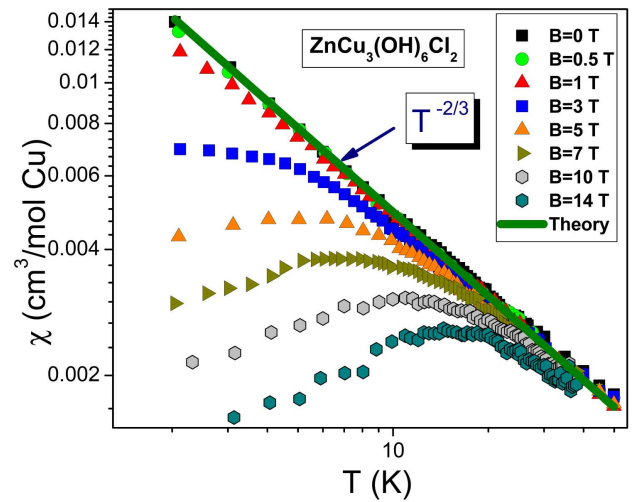


Fig. 2. Measured temperature dependence of the magnetic susceptibility χ of $\text{ZnCu}_3(\text{OH})_6\text{Cl}_2$ from Ref. [10] at magnetic fields shown in the legend. Illustrative values of χ_{\max} and T_{\max} at $B = 3$ T are also shown. A theoretical calculation at $B = 0$ is plotted as the solid line, which represents $\chi(T) \propto T^{-\alpha}$ with $\alpha = 2/3$ [6, 18, 21].

To examine the impurity model of herbertsmithite (see above) in a broader context, we first refer to the experimental behavior of its magnetic susceptibility χ . It is seen from Fig. 2 that the magnetic susceptibility diverges as $\chi(T) \propto T^{-2/3}$ in magnetic fields $B \leq 1$ T, as shown by the solid line. In the case of weakly interacting impurities it has been suggested that the low-temperature behavior of χ can be approximated by a Curie–Weiss law [16, 24, 25], i.e., $\chi_{\text{CW}}(T) \propto 1/(T + \theta)$, with θ a vanishingly small Weiss temperature. However, given the documented behavior $\chi(T) \propto T^{-2/3}$ at low B , the Curie–Weiss approximation is in conflict with both experiment [10] and theory [6, 18, 20]. Moreover, as seen in Fig. 3, the normalized spin susceptibility behaves like the normalized heat capacity extracted from the measurements on YbRh_2Si_2 in high magnetic fields [46].

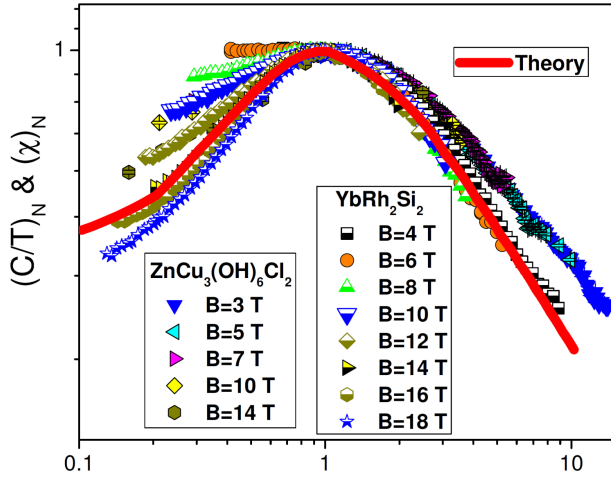


Fig. 3. Normalized susceptibility $\chi_N = \chi/\chi_{\max} = M_N^*$ versus normalized temperature T_N (see Eq. (7)) extracted from the measurements reported in Fig. 2. The normalized specific heat $(C/T)_N = M_N^*$ is extracted from the measurements of C/T on YbRh_2Si_2 in magnetic fields B (legend) [46]. Our calculations made at $B \simeq B^*$ when the quasiparticle band is fully polarized are depicted by the solid curve tracing the scaling behavior of M_N^* [6, 20].

This observation confirms the absence of the spin gap in $\text{ZnCu}_3(\text{OH})_6\text{Cl}_2$ and the consequent invalidity of the impurity model, which artificially separates the contributions coming from the impurities. Within the framework of the impurity model, the calculated intrinsic spin susceptibility of the kagome plane is decomposed as $\chi_{\text{kag}}(T) = \chi(T) - \chi_{\text{CW}}(T)$, leading to $\chi_{\text{kag}}(T \rightarrow 0) \rightarrow 0$ and the erroneous claim that a putative gap has been detected [25]. Thus, we must conclude that the impurity model is untenable, since it cannot explain the empirically established behavior $\chi(T) \propto T^{-2/3}$ [10]. To explain the observed behavior of χ , it is necessary to consider the impurities embedded in the kagome planes of a host crystal as an *integral* system [3, 6, 18–21, 23, 47, 48] that acts coherently to produce additional frustration of the kagome planes, so as to make the QSL robust at lower temperatures. Based on this analysis, we predict that the QSL of quantum magnets can be stabilized introducing a random distribution of impurities.

In a similar vein, working within the impurity model, the authors of Ref. [16] obtain a measure $S_{\text{kag}}(\omega) = S_{\text{tot}}(\omega) - aS_{\text{imp}}(\omega)$ of the intrinsic scattering. This has been done by subtracting the impurity scattering contribution $S_{\text{imp}}(\omega)$ from the total scattering $S_{\text{tot}}(\omega)$, taking a as a fitting parameter. On finding that $S_{\text{kag}}(\omega)$ goes to zero as ω decreases below the energy of 0.7 meV (see Fig. 4b of Ref. [16]) they assert the existence of a gap. However, as we have demonstrated above, such a subtraction leads to the erroneous conclusion that a putative gap has been found. Indeed, this conclusion relies completely on the theoretical assumption that the impurities are weakly interacting; accordingly, it cannot be considered as empirically authenticated, since the subtraction

hypothesis is negated by the experimental behavior summarized in Fig. 2. All relevant experimental observations are consistent with the hypothesis that the properties of $\text{ZnCu}_3(\text{OH})_6\text{Cl}_2$ under study are determined by a stable SCQSL: (i) there is no appreciable gap in the spectrum of spin excitations, such a gap being absent even under the application of high magnetic fields of 18 T, and (ii) the impurity model is untenable from the experimental standpoint.

4. Asymmetric conductivity of heavy-fermion compounds

Direct experimental studies of quantum phase transitions in HTSC and HF metals are of great importance for understanding the underlying physical mechanisms responsible for their anomalous properties. However, such studies of HF metals and HTSC are difficult since the corresponding critical points are usually concealed by the proximity to other phase transitions, commonly antiferromagnetic and/or superconducting. Recently, extraordinary properties of tunneling conductivity in the presence of a magnetic field were observed in a graphene preparation having a flat band [9], as well as in HTSC's and the HF metal YbRh_2Si_2 [7, 8].

Most of the experiments on HF metals and HTSC's explore their thermodynamic properties. However, it is equally important to determine other properties of these strongly correlated systems, notably quasiparticle occupation numbers $n(p, T)$ as a function of momentum p and temperature T . These quantities are not linked directly to the density of states (DOS) $N(\varepsilon = 0)$ determined by the quasiparticle energy ε) or to the behavior of the effective mass M^* . When C and T symmetries are not preserved, the differential tunneling conductivity and dynamic conductance are no longer symmetric functions of the applied voltage V . Since the time-reversal invariance and particle-hole symmetry remain intact in normal Fermi systems, the differential tunneling conductivity and dynamic conductance are symmetric functions of V . Thus, a conductivity asymmetry is not observed in conventional metals at low temperatures.

To determine the tunneling conductivity, we first calculate the tunneling current $I(V)$ through the point contact between two metals. This is done using the method of Harrison [49, 50], based on the observation that $I(V)$ is proportional to the particle transition probability introduced by Bardeen [51]. Bardeen considered the probability P_{12} of a particle (say an electron) making a transition from a state 1 on one side of the tunneling layer to a state 2 on the other side. This quantity has the behavior $P_{12} \sim |t_{12}|^2 N_2(0) n_1(1 - n_2)$ in terms of the density of states $N_2(0)$ (at $\varepsilon = 0$) in state 2, the electron occupation numbers $n_{1,2}$ in these states, and a transition matrix element t_{12} . The total tunneling current I is then proportional to the difference between the current from 1 to 2 and that from 2 to 1, with the result taking the form

$$\begin{aligned}
 I &\sim P_{12} - P_{21} \sim |t_{12}|^2 N_1(0)N_2(0) \\
 &\times [n_1(1 - n_2) - n_2(1 - n_1)] = \\
 &|t_{12}|^2 N_1(0)N_2(0)(n_1 - n_2). \quad (10)
 \end{aligned}$$

Harrison applied the WKB approximation to calculate the matrix element, $t_{12} = t(N_1(0)N_2(0))^{-1/2}$, where t denotes the resulting transition amplitude. Multiplication of expression (10) by 2 to account for the electron spin and integration over the energy ε leads to the total (or net) tunneling current [49, 50]:

$$I(V) = 2|t|^2 \int [n_F(\varepsilon - V) - n_F(\varepsilon)] d\varepsilon. \quad (11)$$

Here $n_F(\varepsilon)$ is the electron occupation numbers for a metal in the absence of a FC, and we have adopted atomic units $e = m = \hbar = 1$, where e and m are the electron charge and mass, respectively. Since temperature is low, $n_F(\varepsilon)$ can be approximated by the step function $\theta(\varepsilon - \mu)$, where μ is the chemical potential.

We note that a more rigorous consideration of the densities of states N_1 and N_2 entering Eq. (10) for $\varepsilon = 0$ requires their inclusion in the integrand of Eq. (11) [52–54]. (For example, see Eq. (7) of Ref. [54], where this refinement has been carried out for the system of a magnetic adatom and scanning tunneling microscope tip.) However, this complication does not break the $I(V)$ symmetry in LFL case. On the other hand, it will be seen below that if the system hosts a FC, the presence of the density-of-states factors in the integrand of Eq. (11) acts to promote the asymmetry of tunneling spectra, for the density of states strongly depend on $\varepsilon = 0$, see Fig. 4.

It follows from Eq. (11) that quasiparticles with single-particle energies ε in the range $\mu - V \leq \varepsilon \leq \mu$ contribute to the current, while $I(V) = c_1 V$ and $\sigma_d(V) \equiv dI/dV = c_1$, with $c_1 = \text{const.}$ Thus, in the framework of LFL theory the differential tunneling conductivity $\sigma_d(V)$, being a constant, is a symmetric function of the voltage V , i.e., $\sigma_d(V) = \sigma_d(-V)$. In fact, the symmetry of $\sigma_d(V)$ holds provided C and T symmetries are observed, as is customary for LFL theory. The symmetry of $\sigma_d(V)$ is therefore quite obvious and common in case of contact of two ordinary metals (without a FC), regardless whether they are in a normal or superconducting state. On the other hand, it will be seen below that if the system hosts a FC, the presence of the density-of-states factors in the integrand of Eq. (11) acts to promote the asymmetry of tunneling spectra.

Indeed, the situation becomes quite different in the case of a strongly correlated Fermi system in the vicinity of a FCQPT that engenders a flat band [39, 40] while violating the C and T symmetries [3, 6]. Part (a) of Fig. 4 illustrates the resulting low-temperature single-particle energy spectrum $\varepsilon(\mathbf{k}, T)$. Part (b), which displays the momentum dependence of the occupation numbers $n(\mathbf{k}, T)$ in such a system, shows that the flat band induced by the FCQPT does in fact entail the violation of C and T symmetries, as reflected in the asymmetry of the regions occupied by particles (labeled p) and by

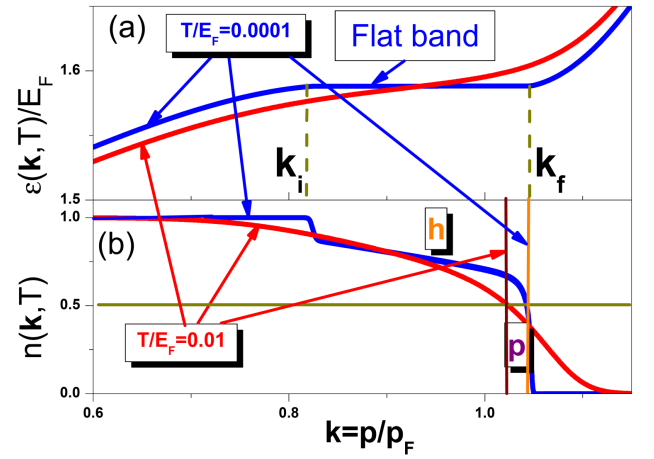


Fig. 4. Flat band induced by FC. The single-particle spectrum (a) and the quasiparticle occupation numbers (b) at small but finite temperatures versus the dimensionless momentum $k = p/p_F$, where p_F is the Fermi momentum. Temperature is measured in the units of E_F . At $T = 0.01E_F$ and $T = 0.0001E_F$ the vertical lines show the position of the Fermi level E_F at which $n(\mathbf{k}, T) = 0.5$ (see the horizontal line in part (b)). At $T = 0.0001E_F$ (blue curve), the single-particle spectrum $\varepsilon(\mathbf{k}, T)$ is almost flat (marked “Flat band”) in the range $k_f - k_i$ (with k_i and k_f denoting respectively the initial and final momenta for FC realization). The distribution function $n(\mathbf{k}, T)$ becomes more asymmetric with respect to the Fermi level E_F , generating the NFL behavior and both C- and T-invariances are broken. To illuminate the asymmetry, the area occupied by quasiholes in part (b) is labeled h (red), that occupied by quasiparticles, by p (red).

holes (labeled h) [3]. It is seen from Fig. 4 that at $T = 0$ the electronic liquid of the system has *two* components. One is an exotic component made up of heavy electrons occupying a range of momenta $p_1 < p < p_2$ (not shown) surrounding the nominal Fermi surface at $p = p_F$. This component is characterized by the superconducting order parameter $\kappa(p) = \sqrt{n(p)(1 - n(p))}$. The other component is made up of normal electrons occupying the momentum range $0 \leq p \leq p_1$; it maintains LFL properties. This unusual momentum-space distribution cannot be described within standard BCS theory; nor can its distinctive properties. In particular, the density of paired charge carriers that form the superfluid density is no longer equal to the total particle density n_{el} represented by paired and unpaired charge carriers. This violation of Leggett’s theorem is to be expected, since both C- and T- invariance are violated in the topologically nontrivial FC state [1, 3, 6].

We are proposing that for the strongly correlated many-fermion systems in question, the approximate equality $n_s \simeq n_{el}$ that would normally be expected for a real system approximating BCS behavior, must be replaced by the strong inequality $n_s = n_{FC} \ll n_{el}$, where n_{FC} is the density of particles in FC state [35]. This implies that the main contribution to n_s comes from the FC state. Indeed, the wave function Ξ describing the state

of the Cooper pairs as a whole concentrates their associated probability density in the momentum domain the flat band (cf. Fig. 4) such that $|\Xi|^2 \propto n_s$, with $|\Xi|^2 \simeq 0$ outside this area. Being defined by the properties of the FC, this area can be very small, nor does it depend on n_{el} , so it can be expected that $n_s \ll n_{el}$ [35].

It is worth noting that the first studies of the overdoped copper oxides suggested that $n_s \ll n_{el}$, but this was attributed to pair-breaking and disorder [55–57], while recent studies with the measurements on ultra clean samples of $\text{La}_{2-x}\text{Sr}_x\text{CuO}_4$ authenticate the result that $n_s \ll n_{el}$ [32]. It is also relevant that the observed high values of T_c together with the linear dependence $\rho_{s0} \propto T_c$ [32] of the resistivity are not easily reconciled with the pair-breaking mechanism proposed for dirty superconductors. One cannot expect that such a mechanism would be consistent with high values of T_c and the increase of T_c with doping. On balance, the evidence supports the hypothesis of fermion condensation as the underlying physical mechanism of both the unusual properties of overdoped copper oxides and the asymmetry of tunneling conductivity [3, 6, 39, 40].

In case of the strongly correlated Fermi system with a FC, the tunneling current becomes [1, 3, 4]:

$$I(V) = 2|t|^2 \int [n(\varepsilon - V, T) - n_F(\varepsilon, T)] d\varepsilon. \quad (12)$$

Here one of the distribution functions of ordinary metal n_F in the right side of Eq. (11) is replaced by $n(\varepsilon, T)$, shown in Fig. 4b. As a result, the asymmetric part of the differential conductivity $\Delta\sigma_d(V) = \sigma_d(V) - \sigma_d(-V)$ becomes finite and we obtain [1–4, 6]:

$$\Delta\sigma_d(V) \simeq c \left(\frac{V}{2T} \right) \frac{p_f - p_i}{p_F}, \quad (13)$$

where c is a constant of order unity. It is worthy noting that Eq. (13) is also valid if the density of states N_1 and N_2 are taken into account, for that only changes c . Note that the conductivity $\Delta\sigma_d(V)$ remains asymmetric also in the superconducting phase of both HTSC and HF metals. In such cases it is again the occupation numbers $n(\mathbf{p})$ that is responsible for the asymmetric part of $\Delta\sigma_d(V)$, since this function is not appreciably disturbed by the superconductive pairing. This is because superconductive pairing is usually weaker than that of Landau in forming the function $n(\mathbf{p})$ [3, 6]. As a result, $\Delta\sigma_d(V)$ remains approximately the same below the superconducting T_c [3].

Under application of a magnetic field B at sufficiently low temperatures $k_B T \lesssim \mu_B B$ (k_B and μ_B are the Boltzmann constant and the Bohr magneton, respectively), the strongly correlated Fermi system transits from the NFL to the LFL regime [3]. As we have seen above, the asymmetry of the tunneling conductivity vanishes in the LFL state [1–4].

Figure 5 shows the differential conductivity σ_d observed in measurements on YbRh_2Si_2 [7, 8]. It is seen that its asymmetry diminishes with elevation of the magnetic field B , as the minima of the curves shift to the $V = 0$ point. (See Fig. 6 for details.) The magnetic

field is applied along the hard magnetization direction, $B \parallel c$, with $B_c \simeq 0.7$ T [8], where B_c is the critical field suppressing the antiferromagnetic order [58]. The asymmetric part of the tunneling differential conductivity, $\Delta\sigma_d(V)$, is displayed in Fig. 6, being extracted from measurements shown in Fig. 5. It is seen that $\Delta\sigma_d(V)$ decreases as B increases. We predict that application of the magnetic field in the easy magnetization plane, $B \perp c$ with $B_c \simeq 0.06$ T, leads to a stronger suppression of the asymmetric part of the conductivity, observing that in this case the magnetic field effectively suppresses the antiferromagnetic order and the NFL behavior.

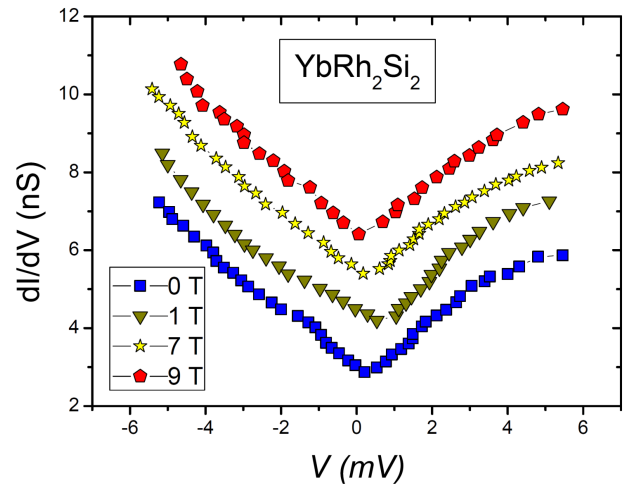


Fig. 5. Differential conductivity $\sigma_d(V) = dI/dV$ measured on YbRh_2Si_2 under the application of magnetic field (legend) along the hard magnetization direction [8].

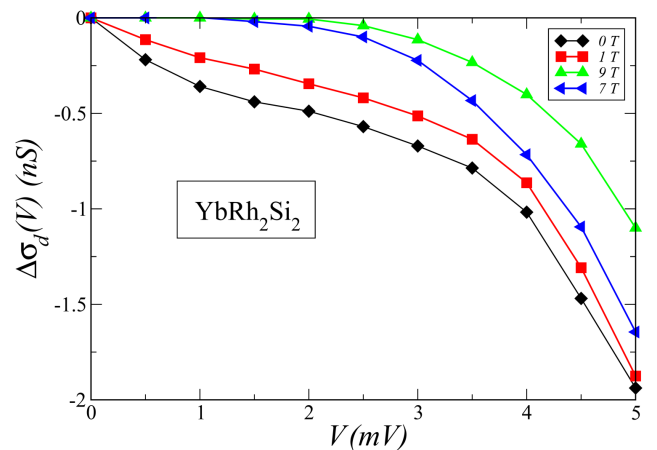


Fig. 6. Asymmetric parts $\Delta\sigma_d(V)$ of the tunneling differential conductivity measured on YbRh_2Si_2 and extracted from the data shown in Fig. 5.

On measuring the differential resistance dV/dI as a function of current I , one finds that its symmetry properties are the same as those of $\sigma_d(V)$; namely, under the application of a magnetic field, the asymmetry

of the differential resistance vanishes as the system transits to a normal Fermi-liquid state. The differential resistance dV/dI of graphene as a function of a direct current I for different magnetic fields B is reported in Fig. 7 [9]. The asymmetric part of the differential resistance $As(I) = dV/dI(I) - dV/dI(-I)$ is seen to diminish with increasing magnetic field, vanishing near $B \simeq 140$ mT. Such behavior is extremely compelling, since the strongly correlated graphene sample has a perfect flat band, implying that the FC effects should be clearly manifested in this material [9].

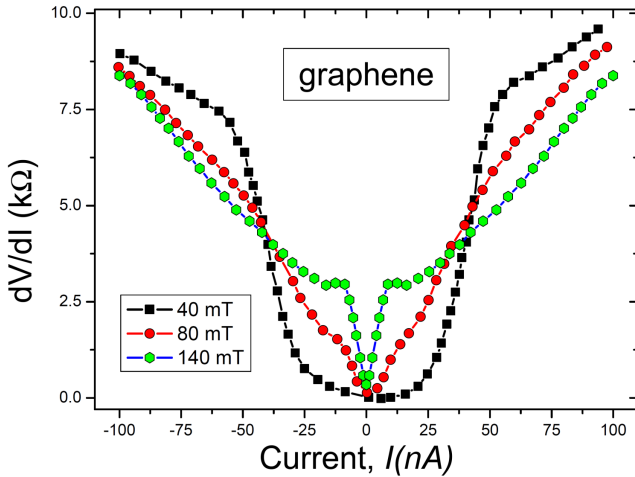


Fig. 7. Differential resistance dV/dI of graphene versus current I at different magnetic fields B shown in the legend [9]. Weak asymmetry is seen at small magnetic fields.

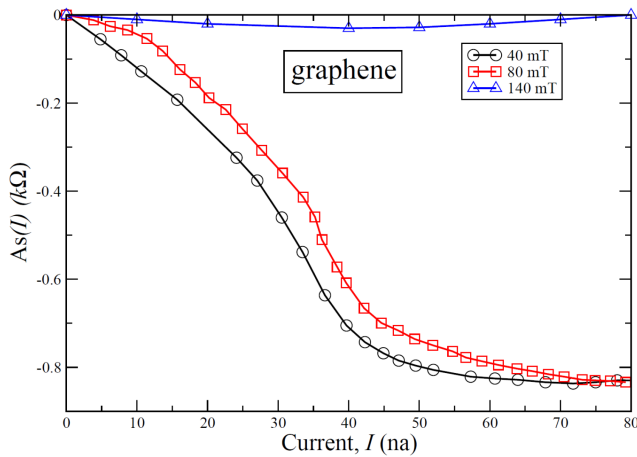


Fig. 8. Magnetic field (legend) dependence of the asymmetric part $dV/dI(I) - dV/dI(-I)$ versus the current I , extracted from the data of Fig. 7 for graphene.

Thus, in accordance with prediction [1–4], the asymmetric part tends to zero at sufficiently high magnetic fields, as is seen from Fig. 8. The asymmetry persists in the superconducting state of graphene [9] and is suppressed at $B \simeq 140$ mT.

Disappearance of the asymmetric part of the differential conductivity in Fig. 8 indicates that as the magnetic field increases, graphene transits from the NFL to the LFL state. To support this statement, we surmise that the resistance $\rho(T)$ should exhibit linear dependence $\rho(T) \propto T$ in the normal state at zero magnetic field, while at higher magnetic fields and low temperatures $k_B T \ll \mu_B B$, the resistance becomes a quadratic function of temperature $\rho(T) \propto T^2$, as is generally the case in other strongly correlated Fermi systems [3, 6].

5. Universal scaling relation for high- T_c superconductors

Another experimental result [36] providing insight into the NFL behavior of strongly correlated Fermi systems is the universal scaling relation, which can also be explained using the flat band concept. The authors of Ref. [36] measured the temperature dependence $d\rho/dT$ of the resistivity ρ for a large number of HTSC substances for $T > T_c$. They discovered quite remarkable behavior: for all substances considered, $d\rho/dT$ shows a linear dependence on $\lambda^2(T=0) \equiv \lambda_0^2$, where λ is the London penetration depth. All of the superconductors considered belong to the London type, for which $\lambda \gg \xi_0$, where ξ_0 is the zero-temperature coherence length (see, e.g., Ref. [35]).

It has been shown that the scaling relation [36]

$$\frac{d\rho}{dT} \propto \frac{k_B}{\hbar} \lambda_0^2 \quad (14)$$

remains valid over several orders of magnitude in λ_0 , signifying its robustness. At the phase transition point $T = T_c$, relation (14) yields the well-known Holms law [36] (see also [59] for its theoretical derivation):

$$\sigma T_c \propto \lambda_0^{-2}, \quad (15)$$

in which $\sigma = \rho^{-1}$ is the normal state dc conductivity. It has been shown by Kogan [59] that the Holms law applies even for the oversimplified model of an isotropic BCS superconductor. Within the same model of a simple metal, one can express the resistivity ρ in terms of microscopic substance parameters [60]: $e^2 n \rho \simeq p_F / (\tau v_F)$, where τ is the quasiparticle lifetime, n is the carrier density, and v_F is the Fermi velocity. Taking into account that $p_F / v_F = M^*$, we arrive at the expression

$$\rho = \frac{M^*}{n e^2 \tau}, \quad (16)$$

which formally agrees with the Drude formula. It has been shown in Ref. [35] that good agreement with experimental results [32] is achieved when the effective mass and the superfluid density are attributed to the carriers in the FC state only, i.e., $M^* \equiv M_{FC}$ and $n \equiv n_{FC}$. Keeping this in mind and utilizing the relation $1/\tau = k_B T / \hbar$ (see Ch. 9 of Ref. [6]), we obtain

$$\rho = \frac{M_{FC}}{e^2 n_{FC}} \frac{k_B T}{\hbar} \equiv 4\pi \lambda_0^2 \frac{k_B T}{\hbar}, \quad (17)$$

i.e. $d\rho/dT$ is indeed given by the expression (14). Equation (17) demonstrates that fermion condensation can explain all the above experimentally observed universal

scaling relations. It is important to note that the FC approach presented here is insensitive to and transcends the microscopic, non-universal features of the substances under study. This is attributed to the fact that the FC state is protected by its topological structure and therefore represents a new class of the Fermi liquids [6, 40]. In particular, consideration of the specific crystalline structure of a compound, its anisotropy, its defect composition, etc. do not change our predictions qualitatively. This strongly suggests that the FC approach provides a viable theoretical framework for explaining universal scaling relations similar to those discovered in the experiments of Božović et al. [32] and Hu et al. [36]. In other words, the fermion condensation of charge carriers in the considered strongly correlated HTSC's, engendered by a quantum phase transition, is indeed the primary physical mechanism responsible for their observable universal scaling properties. This mechanism can be extended to a broad set of substances with a very different microscopic characteristics, as discussed in detail in Refs. [3, 6].

5. Conclusions

The central message of the present paper is that if the electronic spectrum of a substance happens to feature a dispersionless part related to the fermion condensation (FC), or “flat bands”, it is just this aspect that is responsible for measured properties that depart radically from those of familiar condensed-matter systems described by the Landau–Fermi liquid theory. As we have demonstrated above, this is the case irrespective of varied microscopic details characterizing these substances such as crystal symmetry, dimensionality, and defect structure. The explanation for this finding lies in the fact that FC most readily occurs in substances hosting flat bands. Experimental manifestations of FC phenomena are varied, which implies that different experimental techniques are most suitable for detecting and analyzing them.

One example of FC experimental manifestation is the quantum spin-liquid physics in geometrically frustrated magnets and in herbertsmithite in particular. Here we suggest that to elucidate the QSL properties in latter substance, it is essential to perform the targeted measurements of heat transport, low-energy inelastic neutron scattering and optical conductivity in the presence of magnetic fields at low temperatures. Moreover, we have suggested that the increasing x , i.e. the percentage of Zn sites that are occupied by Cu, can facilitate the frustration of the lattice and thereby act to stabilize the QSL state. This conjecture can be tested in experiments on samples of herbertsmithite with different x under the application of a magnetic field. While making a step towards confirmation of the existence of a robust QSL state in herbertsmithite, our considerations may also provide an effective strategy for analyzing this state in the other magnetic insulators having geometrical frustration.

The other important experimental technique is scanning tunneling microscopy, which has the advantage of being sensitive both to the density of states and quasiparticle occupation numbers. The reason for this dual sensitivity is that this technique is a well suited to studying effects related to the violation of particle–hole symmetry and time-reversal invariance. Their violation leads to asymmetry of the differential tunneling conductivity and resistance to the applied voltage V or current I . Based on the recent experimental results, we have demonstrated that the asymmetric part of both the conductivity and the resistivity vanishes under the application of a magnetic field, as predicted in Refs. [1, 2, 4]. To support our statement regarding the role of broken T-invariance, we have analyzed and discussed recent challenging measurements in overdoped cuprates by Božović and co-authors [32] within the fermion condensation framework. Also within the FC framework, we have described and explained otherwise purely empirical observations of scaling properties [36]. Finally, our study of such recent experimental results strongly suggests that the fermion condensation quantum phase transition is an intrinsic feature of many strongly correlated Fermi systems and can be viewed as the universal agent of their non-Fermi-liquid behavior.

Acknowledgments

This work is supported by the National Science Center in Poland as a research project No. DEC-2017/27/B/ST3/02881.

References

- [1] V.R. Shaginyan, *JETP Lett.* **81**, 222 (2005).
- [2] V.R. Shaginyan, K.G. Popov, *Phys. Lett. A* **361**, 406 (2007).
- [3] V.R. Shaginyan, M.Ya. Amusia, A.Z. Msezane, K.G. Popov, *Phys. Rep.* **492**, 31 (2010).
- [4] V.R. Shaginyan, K.G. Popov, V.A. Stephanovich, E.V. Kirichenko, *J. Alloys Comp.* **442**, 29 (2007).
- [5] G.E. Volovik, *Springer Lecture Notes in Physics* **718**, 31 (2007).
- [6] M.Ya. Amusia, K.G. Popov, V.R. Shaginyan, V.A. Stephanovich, *Theory of Heavy-Fermion Compounds*, Springer Series in Solid-State Sciences, Vol. 182, Springer, Heidelberg 2015.
- [7] S. Ernst, S. Kirchner, C. Krellner, C. Geibel, C.G. Zwicknagl, F. Steglich, S. Wirth, *Nature* **474**, 362 (2011).
- [8] S. Seiro, L. Jiao, S. Kirchner, S. Hartmann, S. Friedemann, C. Krellner, C. Geibel, Q. Si, F. Steglich, S. Wirth, *Nat. Commun.* **9**, 3324 (2018).
- [9] Y. Cao, V. Fatemi, S. Fang, K. Watanabe, T. Taniguchi, E. Kaxiras, P. Jarillo-Herrero, *Nature* **556**, 43 (2018).
- [10] J.S. Helton, K. Matan, M.P. Shores, E.A. Nytko, B.M. Bartlett, Y. Qiu, D.G. Nocera, Y.S. Lee, *Phys. Rev. Lett.* **104**, 147201 (2010).

- [11] J.S. Helton, K. Matan, M.P. Shores, E.A. Nytko, B.M. Bartlett, Y. Yoshida, Y. Takano, A. Suslov, Y. Qiu, J.H. Chung, D.G. Nocera, Y.S. Lee, *Phys. Rev. Lett.* **98**, 107204 (2007).
- [12] M.A. deVries, K.V. Kamenev, W.A. Kockelmann, J. Sanchez-Benitez, A. Harrison *Phys. Rev. Lett.* **100**, 157205 (2008).
- [13] T.H. Han, J.S. Helton, S. Chu, A. Prodi, D.K. Singh, C. Mazzoli, P. Müller, D.G. Nocera, Y.S. Lee, *Phys. Rev. B* **83**, 100402 (2011).
- [14] T.H. Han, S. Chu, Y.S. Lee, *Phys. Rev. Lett.* **108**, 157202 (2012).
- [15] T.H. Han, R. Chisnell, C.J. Bonnoit, D.E. Freedman, V.S. Zapf, N. Harrison, D.G. Nocera, Y. Takano, Y.S. Lee, [arXiv:1402.2693](https://arxiv.org/abs/1402.2693) (2014).
- [16] T.H. Han, M.R. Norman, J.J. Wen, J.A. Rodriguez-Rivera, J.S. Helton, C. Broholm, Y.S. Lee, *Phys. Rev. B* **94**, 060409 (2016).
- [17] H. Yamaguchi, M. Okada, Y. Kono, S. Kittaka, T. Sakakibara, T. Okabe, Y. Iwasaki, Y. Hosokoshi, *Sci. Rep.* **7**, 16144 (2017).
- [18] V.R. Shaginyan, A.Z. Msezane, K.G. Popov, *Phys. Rev. B* **84**, 060401 (2011).
- [19] V.R. Shaginyan, A.Z. Msezane, K.G. Popov, V.A. Khodel, *Phys. Lett. A* **376**, 2622 (2012).
- [20] V.R. Shaginyan, A.Z. Msezane, K.G. Popov, G.S. Japaridze, V.A. Stephanovich, *Europhys. Lett.* **97**, 56001 (2012).
- [21] V.R. Shaginyan, A.Z. Msezane, K.G. Popov, G.S. Japaridze, V.A. Khodel, *Europhys. Lett.* **103**, 67006 (2013).
- [22] H.J. Liao, Z.Y. Xie, J. Chen, Z.Y. Liu, H.D. Xie, R.Z. Huang, B. Normand, T. Xiang, *Phys. Rev. Lett.* **118**, 137202 (2017).
- [23] V.R. Shaginyan, M.Y. Amusia, A.Z. Msezane, K.G. Popov, V.A. Stephanovich, *Phys. Lett. A* **379**, 2092 (2015).
- [24] M. Fu, T. Imai, T.H. Han, Y.S. Lee, *Science* **350**, 655 (2015).
- [25] T. Imai, M. Fu, T.H. Han, Y.S. Lee, *Phys. Rev. B* **84**, 020411(R) (2011).
- [26] M.R. Norman, *Rev. Mod. Phys.* **88**, 041002 (2016).
- [27] Y. Zhou, K. Kanoda, T.K. Ng, *Rev. Mod. Phys.* **89**, 025003 (2017).
- [28] L. Savary, L. Balents, *Rep. Prog. Phys.* **80**, 016502 (2017).
- [29] Z. Feng, Z. Li, X. Meng, W. Yi, Y. Wi, J. Zhang, Y.C. Wang, W. Jiang, Z. Liu, S. Li, F. Liu, J. Luo, S. Li, G.Q. Zheng, Z.Y. Meng, J.W. Mei, Y. Shi, *Chin. Phys. Lett.* **34**, 077502 (2017).
- [30] A.J. Leggett, *J. Stat. Phys.* **93**, 927 (1998).
- [31] A.J. Leggett, *Quantum Liquids*, Oxford Univ. Press, 2006.
- [32] J.I. Božović, X. He, J. Wu, A.T. Bollinger, *Nature* **536**, 309 (2016).
- [33] J. Zaanen, *Nature* **536**, 282 (2016).
- [34] J. Dukelsky, V.A. Khodel, P. Schuck, V.R. Shaginyan, *Z. Phys.* **102**, 245 (1997).
- [35] V.R. Shaginyan, V.A. Stephanovich, A.Z. Msezane, G.S. Japaridze, K.G. Popov, *Phys. Chem. Chem. Phys.* **19**, 21964 (2017).
- [36] T. Hu, Yi. Liu, H. Xiao, G. Mu, Yi-F. Yang, *Sci. Rep.* **7**, 9469 (2017).
- [37] A.N. Bruin, H. Sakai, R.S. Perry, A.P. Mackenzie, *Science* **339**, 804 (2013).
- [38] V.R. Shaginyan, K.G. Popov, V.A. Khodel, *Phys. Rev. B* **88**, 115103 (2013).
- [39] V.A. Khodel, V.R. Shaginyan, *JETP Lett.* **51**, 553 (1990).
- [40] G.E. Volovik, *JETP Lett.* **53**, 222 (1991).
- [41] L.D. Landau, *Sov. Phys. JETP* **3**, 920 (1956).
- [42] E.M. Lifshitz, L.P. Pitaevskii, *Statisticheskaya Fizika (Statistical Physics)*, Pt. 2, Nauka, Moscow 1978 (English translation: Pergamon Press, Oxford 1980).
- [43] D. Pines, P. Nozières, *Theory of Quantum Liquids*, Benjamin, New York 1966.
- [44] P. Coleman, in: *Lectures on the Physics of Highly Correlated Electron Systems VI*, Ed. F. Mancini, American Institute of Physics, New York 2002, p. 79.
- [45] J.W. Clark, M.V. Zverev, V.A. Khodel, *Ann. Phys. (New York)* **327**, 3063 (2012).
- [46] P. Gegenwart, Y. Tokiwa, T. Westerkamp, F. Weickert, J. Custers, J. Ferstl, C. Krellner, C. Geibel, P. Kersch, K.H. Müller, *New J. Phys.* **8**, 171 (2006).
- [47] V.R. Shaginyan, M.Y. Amusia, J.W. Clark, G.S. Japaridze, A.Z. Msezane, K.G. Popov, V.A. Stephanovich, M.V. Zverev, V.A. Khodel, [arXiv:1409.4034](https://arxiv.org/abs/1409.4034) (2014).
- [48] V.R. Shaginyan, V.A. Stephanovich, K.G. Popov, E.V. Kirichenko, *JETP Lett.* **103**, 32 (2016).
- [49] W.A. Harrison, *Phys. Rev.* **123**, 85 (1961).
- [50] G. Deutscher, *Rev. Mod. Phys.* **77**, 109 (2005).
- [51] J. Bardeen, *Phys. Rev. Lett.* **6**, 57 (1961).
- [52] I. Giaever, *Phys. Rev. Lett.* **5**, 147 (1960).
- [53] J. Nicol, S. Shapiro, P.H. Smith, *Phys. Rev. Lett.* **5**, 461 (1960).
- [54] A. Schiller, S. Hershfield, *Phys. Rev. B* **61**, 9036 (2000).
- [55] Y.J. Uemura, G.M. Luke, B.J. Sternlieb, J.H. Brewer, J.F. Carolan, W.N. Hardy, R. Kadono, J.R. Kempton, R.F. Kiefl, S.R. Kretzmann, P. Mulhern, T.M. Riseman, D.L. Williams, B.X. Yang, S. Uchida, H. Takagi, J. Gopalakrishnan, A.W. Sleight, M.A. Subramanian, C.L. Chien, M.Z. Cieplak, Gang Xiao, V.Y. Lee, B.W. Statt, C.E. Stronach, W.J. Kossler, X.H. Yu *Phys. Rev. Lett.* **62**, 2317 (1989).
- [56] Y.J. Uemura, A. Keren, L.P. Le, G.M. Luke, W.D. Wu, Y. Kubo, T. Manako, Y. Shimakawa, M. Subramanian, J.L. Cobb, J.T. Markert *Nature* **364**, 605 (1993).

- [57] C. Bernhard, C. Niedermayer, U. Binninger, A. Hofer, C. Wenger, J.L. Tallon, G.V.M. Williams, E.J. Ansaldo, J.I. Budnick, C.E. Stronach, D.R. Noakes, M.A. Blankson-Mills, *Phys. Rev. B* **52**, 10488 (1995).
- [58] P. Gegenwart, J. Custers, C. Geibel, K. Neumaier, T. Tayama, K. Tenya, O. Trovarelli, F. Steglich, *Phys. Rev. Lett.* **89**, 056402 (2002).
- [59] V.G. Kogan, *Phys. Rev. B* **87**, 220507 (2013).
- [60] A.A. Abrikosov, L.P. Gor'kov, I.E. Dzyaloshinskii, *Methods of Quantum Field Theory in Statistical Physics*, Dover, New York 1975.